LA-UR -98-3149

Approved for public release; distribution is unlimited.

TITLE: DESIGN AND PLACEMENT CONSIDERATIONS FOR PROPELLER-TYPE T-ZERO CHOPPERS

CONF-980680--

AUTHOR(S): R. A. Robinson, LANSCE-12

SUBMITTED TO: ICANS-XIV, (International Collaboration on Advanced Neutron Sources)
14-19 June 1998
Starved Rock IL

Los Alamos
NATIONAL LABORATORY

Form No. 836 R5
ST 2629 10/91

DISCLAIMER

DESIGN AND PLACEMENT CONSIDERATIONS FOR PROPELLER-TYPE T-ZERO CHOPPERS

R. A. Robinson, Los Alamos National Laboratory, Los Alamos, NM 87545

We discuss factors to do with placement and running speeds of "propeller-type" t-zero choppers, as implemented at ISIS (on chopper spectrometers) and at LANSCE (on a reflectometer, chopper spectrometer and small-angle scattering instrument).

Propeller-syle t-zero choppers have been used at spallation sources since the HET chopper spectrometer was originally constructed[1], and similar t-zero choppers have been installed on other chopper instruments[2] at ISIS, as well as on the SPEAR reflectometer, the PHAROS chopper spectrometer[3] and, more recently, the LQD small-angle machine at LANSCE. In all cases, the purpose is to block the burst of high-energy neutrons that emanates from the source when the proton beam strikes the target, and still be fully open when the thermal neutrons of interest pass through the space occupied by the t-zero chopper. In general, roughly 30 cm of high-strength high-Ni alloy (like nimonic or inconel) is placed in the beam, and for background purposes, it is desirable to place the chopper as far upstream as possible. Examples of rotor geometries are shown in Fig. 1, while Fig. 2 is a photograph of the 750 lb inconel rotor used in the PHAROS t-zero chopper.

Table I lists those parameters that are available to perform an optimisation, along with constraints, typical outer bounds and the values actually used on the high-resolution chopper spectrometer PHAROS[3] at LANSCE. As regards materials, we use Inconel X-750 [4], a high-tensile-strength high-nickel alloy (density $\rho = 8.3$ g cm^{-3}; yield strength $\sigma_{yield} = 690$ MPa; fast-neutron mean free path = 3.4 cm) as the neutronic element in our t-zero choppers. Following practice at ISIS, we have used 30 cm of inconel (as measured along the neutron beam path), which corresponds to ~ 8.8 fast-neutron mean free paths. The next constraint to consider is the maximum rotational

and yet have the thermal beam fully open in time for the highest energy neutrons of interest to pass through completely unimpeded. The latter condition is not so straightforward, and the ISIS *t*-zero choppers on HET and MARI are not fully open at 1eV, for instance. If one simply considers a fixed point on the chopper sweeping across the thermal beam of width $d_{thermal}$, the maximum neutron energy E_{max} that can pass through is

$$E_{max}(meV) = 5.22697 \times 10^{-6} \left(\frac{2\pi\nu RL}{d_{thermal}} \right)^2 \qquad (3).$$

The parameters that are available to the instrument designer, for a given desired E_{max} and beam width $d_{thermal}$, are the chopper rotational frequency ν, the chopper radius R and the distance L at which chopper is placed, measured from the source. As an example, Fig. 5 shows a set of frequency-radius curves for different chopper placements, assuming a 10-cm wide beam and the use of neutrons up to 1eV. One needs to be to the upper-right side of these lines, and it is very difficult to achieve this, by placing the chopper at the edge of the biological shield (say at 5m) - it involves either a very large or a very fast rotor. Equations (2) and (3) can now be combined into a very useful rule of thumb for chopper design, because they both have the same $\nu = 1/R$ functional dependence:

$$\frac{d_{thermal}}{2\pi L} \sqrt{\frac{E_{max}(meV)}{5.22697 \times 10^{-6}}} < R\nu < \frac{1}{2\pi} \sqrt{\frac{2\sigma_{yield}}{S\rho}} \qquad (4),$$

or stated another way that is independent of R and ν,

$$L > d_{thermal} \sqrt{\frac{E_{max}(meV)}{5.22697 \times 10^{-6}} \frac{S\rho}{2\sigma_{yield}}} \qquad (5).$$

where s is the degree of overlap on the trailing edge of the chopper blade, and the second line of each equation assumes that the chopper blade is centred on the neutron beam when protons hit the target. **Equation 7 is particularly useful for determining how much overlap one can tolerate, given a desired value of E_{full}.** Of course, for the fast-neutron beam, there are corresponding equations in which $s_{thermal}$ and $d_{thermal}$ are replaced by s_{fast} and d_{fast}.

The overlap s_{fast} (see Fig. 4(c)) also determines how well the chopper and accelerator must be phased to each other, or how much jitter is acceptable in the chopper-accelerator timing-control system:

$$t_{jitter}(\mu s) = \frac{10^6 s_{fast}}{2\pi\nu R} = \frac{10^6 (t - d_{fast})}{4\pi\nu R} \qquad (8)$$

and one can replace s_{fast} and d_{fast} by $s_{thermal}$ and $d_{thermal}$ to give the equivalent fast-neutron jitter.

One also has to choose whether to construct the chopper such that it is *symmetrically* balanced, with the rotor entering the beam every 180°, or *asymmetrically* balanced in such a way that the rotor only re-enters the beam after a full revolution, as shown in Fig. 1(b). This effect is shown schematically in Fig. 7(a), for the PHAROS t-zero chopper parameters, in the time domain. Symmetric choppers are generally undesirable for broad-band cold-neutron applications, because the rotor re-enters the beam at a time corresponding to useful neutron bandwidth, and the uninterrupted wavelength bandwidth can be doubled using an asymmetric rotor - such choppers are used on SPEAR and LQD at LANSCE. However, asymmetric rotors can be more complicated to fabricate and balance. The energies at which the rotor re-enters the beam are

$$E_{180}(\mathrm{meV}) = 5.22697 \times 10^{-6} \left(\frac{2L}{\nu} \right)^2 \qquad (9)$$

It would also be worthwhile to investigate whether it is beneficial to include any other materials, like hydrogenous materials or thermal-neutron absorbers such as boron, cadmium or gadolinium, into the rotor or its surfaces.

Finally, it seems that the actual performance of such choppers has never been measured, and it would be desirable to do so in an experiment with detectors placed before and after the rotor.

ACKNOWLEDGEMENTS

I am grateful for discussion with Mark Taylor and Ben Etuk regarding the mechanical engineering aspects discussed here, and to Phil Seeger and Luc Daemen for useful discussion. This work was supported in part by the division of Basic Energy Sciences of the U.S. Department of Energy under contract number W-7405-ENG-36.

Figure Captions

Figure 1 Schematic diagram showing t-zero choppers as implemented (a) at ISIS, (b) on SPEAR and LQD at LANSCE, and (c) on PHAROS at LANSCE. The neutron-attenuating material is shown by the shading and an alumunium alloy is typically used for the other structural components. (a) and (c) are *symmetrically* balanced, with the rotor entering the beam twice per revolution, while (b) is *asymmetrically* balanced and enters only once per revolution.

Figure 2 Photograph of the rotor for the t-zero chopper on the high-resolution chopper spectrometer PHAROS (see Ref. 3) at LANSCE. The rotor is symmetrically balanced, and the neutron beam passes throught the square sections at the ends of the blades. It is constructed from a set of twelve 25-mm thick plates of Inconel X-750, and weighs 341 kg.

Figure 3 Chopper frequency - radius bounds determined from the yield stress and density of Inconel X-750, using Equation (2) with an engineering safety factor S = 3. In designing the chopper, one must remain on the lower left-hand side of the line. The (+) symbol represents the rotor used on PHAROS.

Figure 4 Schematic diagram showing the thermal and fast-neutron beams for (a) a normal thermal beam using apertures (B_4C) and larger aperture fast-neutron shielding (steel, polyethylene, epoxy resin), and (b) for a guide, in which the fast-neutron aperture is less well-defined. In (a) and (c), some of the symbols used in the text for chopper and beam dimensions are shown.

Figure 5 Chopper frequency - radius bounds determined from the desired maxiumum useful neutron energy E_{max}, beam width $d_{thermal}$ and for source-chopper distance = 5, 10 and 15m, using Equation (3). For the example shown here, we assume E_{max} = 1eV and $d_{thermal}$ = 10 cm. The chopper must operate in the region to the upper right-hand side of the curve.

Figure 6 Plot of closest possible chopper position versus beam size for several neutron energies, following Equation (5). The numbers presented here, which assume the use of Inconel X-750 and a safety factor S = 3, take no account of the overlap of the chopper, beyond the beam size. This effect can be included simply by using s + d in place of d for the beam size in Equation (5).

Figure 7 Calculated neutron-beam transmissions for the PHAROS t-zero chopper (see Tables I and II, and/or Ref. 3, for parameters), assuming that the chopper is completely black and that the both the thermal and fast-neutron apertures are perfect absorbers. The real geometry has been approximated by one in which the edges of the chopper blade are radial from the shaft axis. In (a), the thermal-beam performance of the real symmetric chopper is shown, followed by an equivalent asymmetric chopper and the fast-neutron performance. In (b) the thermal and fast-neutron performance in the region close to t = 0 is shown. Note that the larger fast-neutron beam is fully closed for a shorter time than the thermal beam, in agreement with the values given in Table II.

Table II: Parameters and Characterisics for the t-zero chopper on PHAROS[3] at LANSCE.

Parameter	Symbol	Standard/Thermal	Fast-Neutron
source-chopper distance	L	14 m	
chopper radius	R	350 mm	
chopper rotation frequency	ν	60 Hz	
chopper tip speed	v	132 ms^{-1}	
beam width	d	72.5 mm	96.9 mm
chopper blade width	t	116.0 mm	
Idealised maximum energy	E_{max}	3.39 eV	1.90 eV
Energy at which beam begins opening	E_{start}	37.7 eV	195 eV
Energy at which beam is fully open	E_{full}	1.86 eV	1.47 eV
Energy when other blade re-enters beam	E_{180}	14.75 meV (12.5 - 17.6 meV)	
Energy when original blade re-enters beam	E_{360}	3.69 meV (3.4 - 4.0 meV)	
allowable jitter	t_{jitter} (μs)	165 μs	72.4 μs

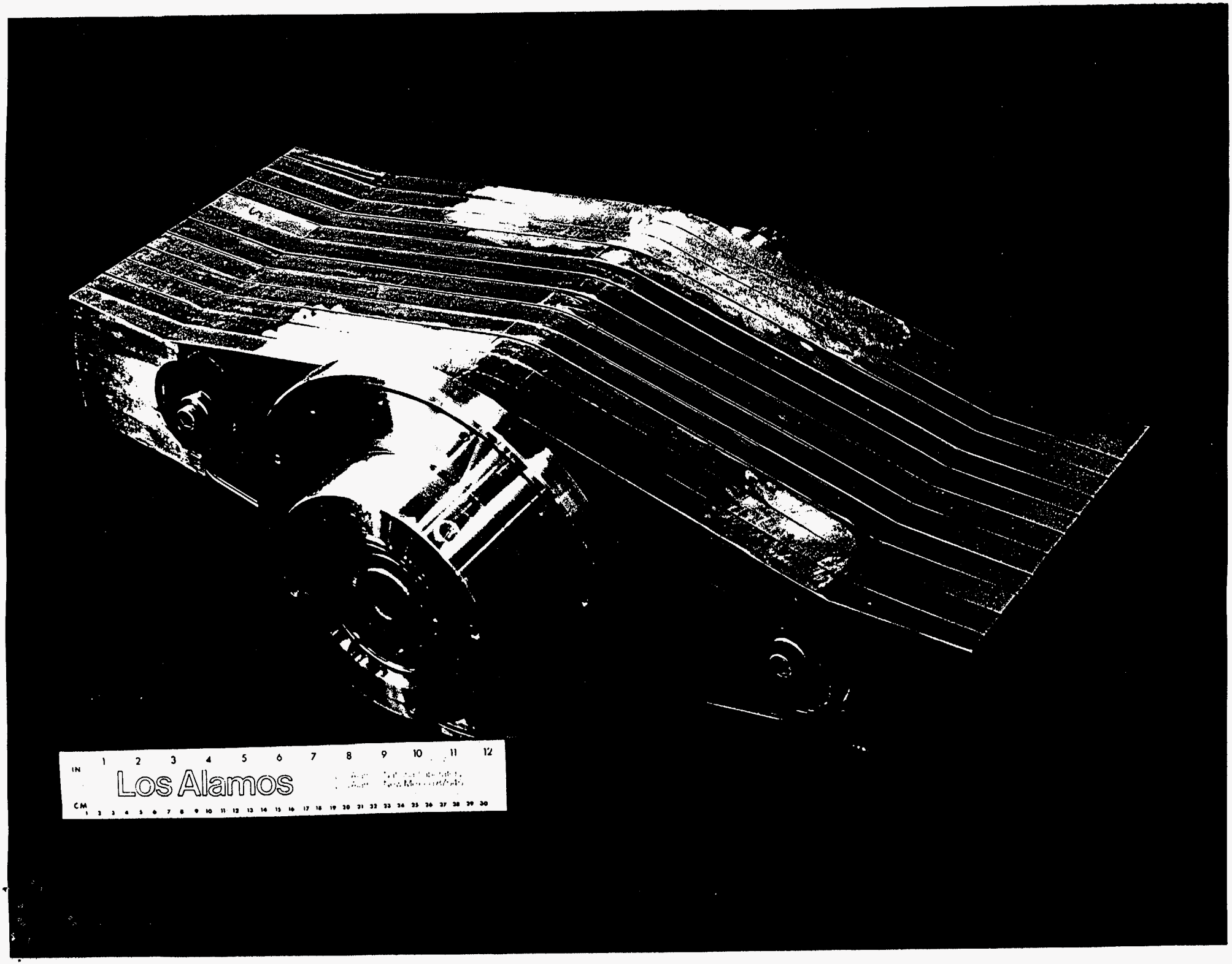
IN 1 2 3 4 5 6 7 8 9 10 11 12
Los Alamos
CM

(a) Thermal beam with apertures

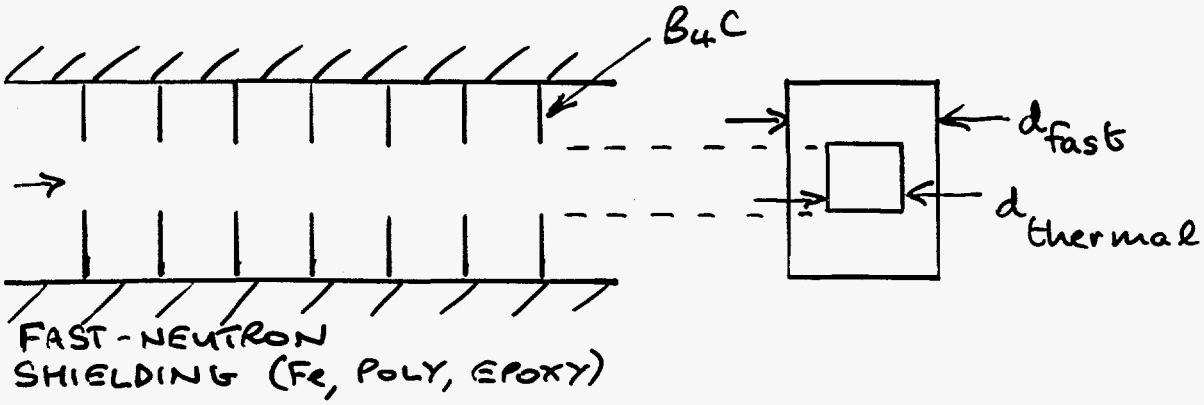

(b) Guide

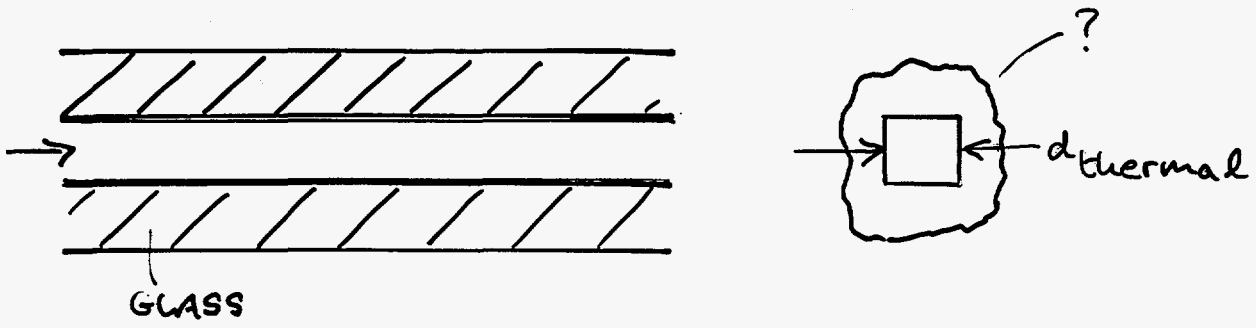

(c) Definitions

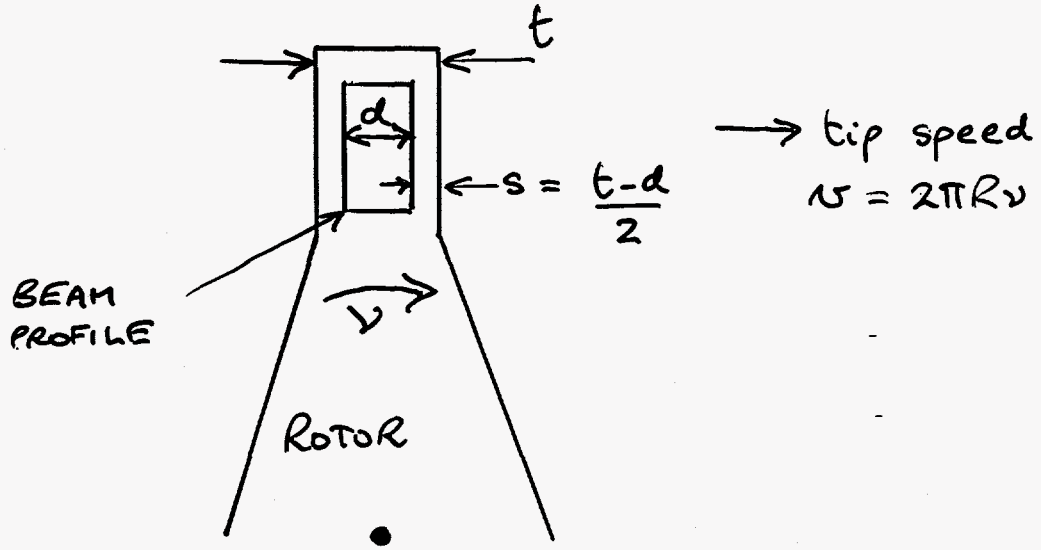

Fig. 6

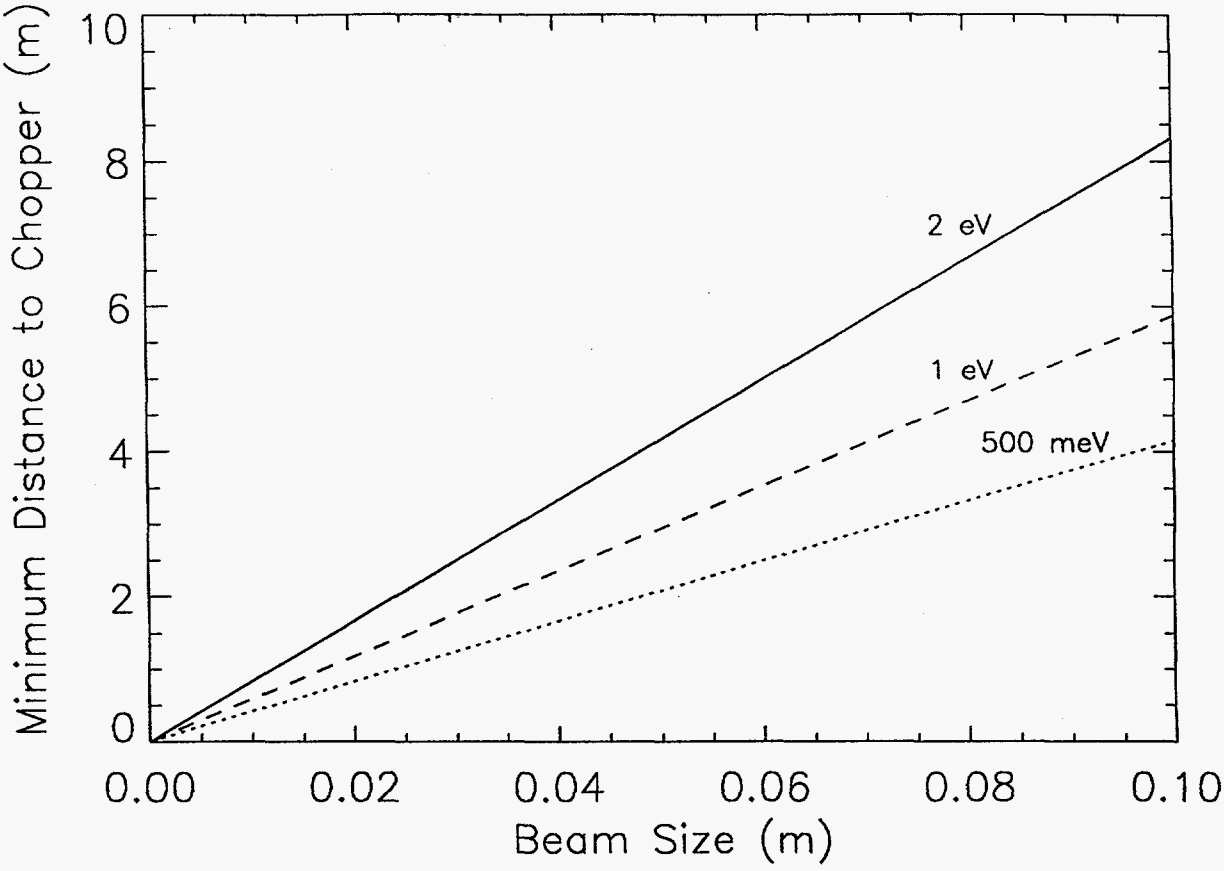
Minimum Distance to Chopper (m)
10
8
6
4
2
0
0.00
0.02
0.04
0.06
0.08
0.10
Beam Size (m)
2 eV
1 eV
500 meV